Self-Consistent Approach to the Structure and Dynamics of T=1 Mirror Nuclei

Abstract

We study the effect of isospin impurity on the superallowed Fermi β decay using the Excited Vampir variational model for the description of the lowest excited 0^+ states in the T=1 nuclei ^{82}Nb and ^{82}Zr, and ^{86}Tc and ^{86}Mo. Results on non-analog β decay branches for the A=82 and A=86 mass nuclei are obtained. The calculated branch for the ^{82}Nb$\rightarrow^{82}$Zr β decay to the first excited 0^+ state with considerable strength is predicted to coexist with the superallowed decay. The structure and electromagnetic properties of the low and high spin isobaric analogue states in ^{82}Nb and ^{82}Zr, as well as ^{86}Tc and ^{86}Mo are presented and compared with available experimental information.

PACS : 21.10.-k; 23.40.-s; 27.50.+e; 21.60.n

Keywords : Nuclear structure; Shape coexistence; Proton-rich mirror nuclei; Superallowed β decay; Isospin mixing.

1. Introduction

The investigation of the structure of exotic nuclei around the N=Z line in the $A \simeq 80$ mass region is one of the most exciting challenges in low energy physics today. Apart from displaying some rather interesting nuclear structure effects these nuclei play an important role in weak interaction and nuclear astrophysics since the abundence flow of the rapid proton capture process (rp process) is determined mainly by the competition of proton capture reactions and β decays along the N=Z line. Recent reaction network calculations have shown that the rp process ends in a closed SnSbTe cycle [1]. Since the detailed reaction rates depend on the nuclear structure, information on the low-lying levels of N$\simeq$Z nuclei is very important.

The charge independence of nuclear forces requires that the energy spectra in pairs of mirror nuclei are identical. Small differences between energy levels could then be interpreted as pure Coulomb effects. Introducing the Coulomb interaction for the valence protons we intend to make a comparison of the microscopic structure of the mirror nuclei ^{82}Zr and ^{82}Nb, and ^{86}Mo and ^{86}Tc.

Superallowed Fermi β decays between analog states provide tests of the validity of the conserved vector current (CVC) hypotesis and the unitarity of the Cabibbo-Kobayashi-Maskawa (CKM) matrix (see [2] and the references therein). Combining the vector coupling constant (G_v) of nucleon β decay with that of the purely leptonic muon decay, the CKM matrix element between u and d quarks (V_{ud}) can be determined. This amplitude together with the mixing amplitudes V_{us} and V_{ub}, provides the possibility to test experimentally the standard three-generation quark model for the electroweak interaction. Intens theoretical effort was devoted in the last years to the investigation of the superallowed beta decay of nuclei with A$\geq$62 [2-7]. Several experimental programs have been recently initiated to measure the half-

lives and branching ratios for the superallowed decays of odd-odd N=Z nuclei with A≥62, where the charge-dependent correction terms are expected to be large.

Two classes of nucleus-dependent corrections must be applied to the measured ft value of a $0^+ \rightarrow 0^+$ β transition between T=1 analog states in order to obtain the coupling constant G_v via the relationship [2]

$$ft(1+\delta_R)(1-\delta_c) = \frac{K}{2G_v^2(1+\Delta_R^v)} \tag{1.1}$$

where f is the statistical rate function, t is the partial half-life for the transition, δ_c is the isospin-symmetry-breaking correction, δ_R is the transition-dependent part of the radiative correction, Δ_R^v is the transition-independent part, and K is a known constant.

In this study we will examine the isospin mixing effect resulting from the variational Excited Vampir approach to the structure of some A≃80 mass nuclei. We report illustrative calculations demonstrating that the deformation effects are growing for nuclei dominated by oblate-prolate shape coexistence on the low-energy spectrum.

Calculations based on the variational approaches of the VAMPIR family have been successfully performed for the description of a variety of nuclear structure phenomena in the A≃70 mass region, not only in nuclei along the valley of β-stability, but also in some exotic nuclei close to the proton drip line [7-19]. The *complex* EXCITED VAMPIR approach allows for a unified description of low and high spin states including in the projected mean fields neutron-proton correlations in both the T=1 and T=0 channels and general two-nucleon unnatural-parity correlations. The oblate-prolate coexistence and mixing, the variation of the deformation with mass number, increasing spin , as well as excitation energy have been compared with the available experimental information. Since the Vampir approaches enable the use of rather large model spaces and of general two-body interactions, *large-scale* nuclear structure studies going far beyond the abilities of the conventional shell-model configuration-mixing approach are possible. Our previous investigations on microscopic aspects of shape coexistence in N≃Z nuclei in the A≃70 mass region indicated the presence of a strong competition between particular configurations based on large and small oblate and prolate quadrupole deformations. Furthermore, as expected, since in N≃Z nuclei neutrons and protons fill the same single particle orbits, the neutron-proton pairing correlations were found to play an essential role [8]. On the other hand the theoretical results suggest that certain properties of these nuclei are extremely sensitive to small variations of particular parts of the effective Hamiltonian [9, 10]. Thus, our results indicate that the oblate-prolate coexistence and mixing at low spins depend on the strengths of the neutron-proton T=0 matrix elements involving nucleons occupying the $0f_{5/2}$, $0f_{7/2}$ and $0g_{9/2}$ single particle orbits.

Since our microscopic investigations on the coexistence phenomena in this mass region have already passed many experimental tests, we thought it worthwhile to apply the same methods to study the effect of isospin mixing on superallowed Fermi β decay for the A=82 and A=86 isospin T=1 nuclei. The investigations are extended to the structure of low and high spin isobar analogue states in the two pairs of T=1 nuclei, ^{82}Zr and ^{82}Nb, and ^{86}Mo and ^{86}Tc.

We shall briefly describe the *complex* Excited Vampir variational procedure and define the

effective Hamiltonian in the next section. In Section 3 we shall then discuss the results on isospin mixing corrections for superallowed Fermi β decays involving two pairs of T=1 nuclei: ^{82}Zr, ^{82}Nb, and ^{86}Mo, ^{86}Tc.
Results on the low and high spin states including electromagnetic properties will be compared for the ^{82}Zr and ^{82}Nb, and ^{86}Mo and ^{86}Tc as well as with the available data. Finally we shall present some conclusions in Section 4.

2. Theoretical framework

We calculated the lowest 0^+ states in ^{82}Zr, ^{82}Nb, and ^{86}Mo, ^{86}Tc to investigate the superallowed Fermi β decay of ^{82}Nb and ^{86}Tc.
In order to make a comparison of the structure of low and high spin isobaric analogue states in the A=82 and A=86 nuclei we calculated the positive-parity states up to spin 20^+.
The variational procedure which we use involves projection before variation on particle number, angular momentum and parity, but not on isospin. First the Vampir solutions, representing the optimal mean-field description of the yrast states by single symmetry-projected HFB determinants, have been obtained. Then the Excited Vampir approach was used to construct additional excited states by independent variational calculations. The final solutions have been obtained diagonalizing the residual interaction between the succesively constructed orthogonal configurations.
We define the model space and the effective Hamiltonian as in our earlier calculations for nuclei in the $A \simeq 70$ mass region [19]: a ^{40}Ca core is used and the valence space consists out of the $1p_{1/2}$, $1p_{3/2}$, $0f_{5/2}$, $0f_{7/2}$, $1d_{5/2}$ and $0g_{9/2}$ oscillator orbits for both protons and neutrons. The effective two-body interaction is a renormalized nuclear matter G-matrix based on the Bonn One-Boson-Exchange potential (Bonn A). In the charge dependent Hamiltonian the Coulomb matrix elements for the valence protons and shifts in the proton single particle energies are added. The corresponding shifts are calculated for each mass number using spherical Hartree-Fock calculations based on Gogny force. It is worthwhile to mention a few particular aspects of the renormalization procedure which are relevant to the present investigations. The G-matrix is modified by three short range (0.707 fm) Gaussians for the isospin T=1 proton-proton, neutron-neutron and neutron-proton matrix elements with strengths of - 35 MeV. The isoscalar spin 0 and 1 particle-particle matrix elements are enhanced by an additional Gaussian with the same range and the strength of -70 MeV. In addition, the interaction contains monopole shifts of -400 keV for all the diagonal isospin T=0 matrix elements of the form $\langle 0g_{9/2}0f; IT=0|\hat{G}|0g_{9/2}0f; IT=0\rangle$ with $0f_{5/2}$ and -250 keV for the $0f_{7/2}$ ones, and shifts of -500 keV in the $\langle 1p1d_{5/2}; IT=0|\hat{G}|1p1d_{5/2}; IT=0\rangle$ matrix elements, where 1p denotes either the $1p_{1/2}$ or the $1p_{3/2}$ orbit. These shifts have been introduced in our earlier calculations in order to influence the onset of deformation. We have to mention that it is the best renormalization of the G-matrix which we obtained in the last years and was successfully used for the description of the Gamow-Teller β decay of proton-rich nuclei in this mass region. More data on the electromagnetic properties of

the nuclei in this mass region, as well as β decay properties justify a new endeavour on the renormalization procedure starting from the Bonn CD which includes charge symmetry breaking and charge independence breaking.

3. Results and discussion

3.1 Superallowed β decay

The β^+-decay half-lives for the heaviest N=Z nuclei, ^{82}Nb and ^{86}Tc, for which Fermi super-allowed decays have been established, have been measured following the fragmentation of a primary ^{92}Mo beam at GANIL, France [20]. The experimental half-live is 52(6) ms for ^{82}Nb and 45(12) ms for ^{86}Tc.

For the description of the investigated 0^+ states in ^{82}Zr and ^{82}Nb and ^{86}Mo and ^{86}Tc in the final diagonalization up to 13 projected configurations were taken into account.

In ^{82}Zr and ^{82}Nb the first two minima are prolate deformed while in the ^{86}Mo and ^{86}Tc already the second minimum is oblate deformed in the intrinsic system. The results obtained for the A=82 as well as A=86 nuclei indicate a variable, sometimes very strong, mixing of prolate and oblate deformed configurations in the final wave functions. We should mention that for this 13 (12)-dimensional many-nucleon basis used in the present calculation the lowest 13 (12) 0^+ states are spread over 6.5 MeV excitation energy in both ^{82}Zr and ^{82}Nb (^{86}Mo and ^{86}Tc).

Concerning the Q_{EC} calculated values are in good agreement with the present evaluated results. For the ^{82}Nb β decay the theoretical result is 10.583 MeV compared with 11.220 (0.592) MeV [21]. For the decay of ^{86}Tc the calculations give 10.803 MeV, while the value extracted from systematic trends is 11.350 (0.532) MeV [21].

Using these Excited Vampir wave functions we calculated the transition strengths for the analog and non-analog branches of the Fermi β decay. The results obtained for ^{82}Nb$\rightarrow^{82}$Zr decay presented in Fig.1 indicate that the upper limit for the isospin mixing is 2.0% and the lower limit is 1.0% with the 13 dimensional many-nucleon basis used in the present investigation. A non-analog branch with an upper limit of 1.4% and a lower limit of 0.4% is found to take place to the first-excited 0^+ state situated at 1.9 MeV excitation energy. This strong branch prediction is a hint for possible experimental investigation.

The results obtained for the ^{86}Tc$\rightarrow^{86}$Mo decay presented in Fig. 2 indicate that the upper limit for the isospin mixing is 1.2% and the lower limit is 0.2%. The missing strength is distributed over the 0^+ excited states.

The results reported here represent the first calculations of this type able to estimate the significant non-analog strengths for the A=82 and A=86 nuclei. In order to extract a more reliable value of the isospin mixing correction more effort will be devoted in the near future for improving the accuracy of the wave functions of the involved 0^+ states increasing considerably the dimension of the Excited Vampir many-nucleon basis.

In the frame of the Excited Vampir approach the many-body wave functions for the involved

0^+ states are independently calculated applying the projection before the variation for each considered nucleus. All the investigated effects should be described by the corresponding wave functions if the many-nucleon basis is large enough and the effective interaction is adequate for the employed model space in a given mass region.

3.1 Low- and high-spin states in T=1 mirror nuclei

Coexistence of two or more stable shapes at comparable excitation for a given spin and parity has been known in the A$\simeq$70 mass region. The most deformed nuclei in the region have been observed for Z number 38 and 40. A marked change in structure was expected around N=44, approaching the spherical shell gap at N=50. The N$\simeq$Z niobium, molybdenum, and technetium isotopes lie between Z=40 and N=50 and the competition between the prolate and oblate deformation is to be expected. Low- and high-spin states in the T=1 mirror nuclei ^{82}Nb and ^{82}Zr, as well as ^{86}Tc and ^{86}Mo are presently investigated in order to predict the differences between the isobaric analogue states with increasing spin. The oblate-prolate shape-coexistence as well as shape-mixing phenomena are studied in the frame of the *complex* Excited Vampir approach. The available data suggest that ^{82}Zr exibit shape coexistence [22]. With rapid changes in collectivity nearby, the N=44 isotones with Z$\geq$40 are expected still to exhibit rotational structures [23]. We calculated the lowest 8 states of positive parity up to spin 20^+ in ^{82}Zr. For ^{82}Nb the lowest 2^+ and 4^+ states have been investigated using an 8 dimentional Excited Vampir basis, while for the higher spin states only the lowest three configurations have been constructed. In ^{82}Zr the lowest two states at each spin are prolate deformed and then appears the first oblate projected configuration. The yrast state for each investigated spin is built out of the lowest configuration, but for the yrare states a variable, sometimes strong mixing was obtained. The states have been organized in bands according to the B(E2) values connecting them. In Fig. 3 we present the ^{82}Zr spectrum and in Table 1 the B(E2) values for the yrast band compared with the available data [22]. In Fig. 4 we present the calculated spectrum for ^{82}Nb. A direct comparison of the yrast positive-parity band in the two mirror nuclei are presented in Fig. 5. The irregularities observed in the data for ^{82}Zr are also seen in the theoretical spectrum at spins 12^+ and 18^+, as well as in ^{82}Nb. Good agreement with the data is obtained for the B(E2) values as can be observed from Table 1, which indicates also similar quadrupole deformation for the two mirror nuclei. In Figs. 6 and 7 we present the alignment plot and the $0g_{9/2}$ occupations, respectively for the states presented in the spectrum in Fig. 3. The alignment plot indicates that protons are aligning first from spin 10^+ to 12^+ and above spin 12^+ also neutrons are aligning fast. In Figs. 8 and 9 we present the alignment plot and the $0g_{9/2}$ occupations in ^{82}Nb. This figures indicate that for the yrast states neutrons and protons manifest the same alignment. Correlating the alignment plots in the two mirror nuclei we can not conclude on the importance of the neutron-proton pairing correlations. The prolate-oblate coexistence found in the structure of the lowest 13 0^+ states involved in the analogue and non-analogue superallowed Fermi β decay of ^{82}Nb to ^{82}Zr is corroborated by the presence of this mixing at

low-, intermediate- and high-spin non-yrast states found in both nuclei. The investigation will be extended in the near future increasing the dimension of the many-nucleon Excited Vampir basis in order to increase the accuracy of our predictions.

For the A=86 mirror nuclei ^{86}Mo and ^{86}Tc we calculated the lowest up to 6 Excited Vampir confirgurations for intermediate and high spin positive parity states. For the 0^+ states the lowest 12, for spins 2^+ and 4^+ the lowest 8 Excited Vampir states have been taken into account. Again prolate-oblate coexistence and mixing was found in the non-yrast states up to spin 18^+. In Fig. 10 we present the theoretical spectrum for ^{86}Mo compared with the available data [23]. As in the data irregularities in the yrast rotational spectrum appear at spins 10^+ and 16^+. The B(E2) values presented in Table 2 indicate a smaller deformation for the yrast band in ^{86}Mo with respect to ^{82}Zr, as it is expected. In Fig. 11 we present the theoretical spectrum of ^{86}Tc compared with the available data. In Fig. 12 a direct comparison of the yrast bands of the A=86 mirror nuclei indicates that the irregularity at spin 10^+ takes place in both nuclei, while in ^{86}Tc the second upbend appears at spin14^+ and not 16^+ as in ^{86}Mo. In order to clarify the problem we have to extend the dimension of the Excited Vampir basis. Fig. 13 indicates that the first fast proton alignment occurs at spin 10^+, while at spin 16^+ a fast neutron alignment explain the upbending in the yrast spectrum. The occupations presented in Fig. 14 support the alignment plot. In Fig. 15 the alignment plot for ^{86}Tc is similar with the one observed in ^{82}Nb, neutrons and protons manifest the same behaviour. The $0g_{9/2}$ occupations presented in Fig. 16 corroborate the alignment results.

4. Conclusions

In this report we presented the first results on the effect of isospin mixing on superallowed Fermi β decay for the A=82 and A=86 T=1 nuclei calculating the lowest 0^+ states in these nuclei in the frame of the *complex* Excited Vampir approach using the best effective interaction which we obtained up to now for this mass region. The first theoretical estimation of the strengths of the significant non-analog branches is presented. We have to increase the dimension of the many-nucleon basis used to describe the 0^+ states within the Q_{EC} window. Another refinement of our calculations will be introduced once we shall start from the Bonn CD interaction since in the present calculations the charge symmetry breaking and charge independence breaking have been taken into account only in the renormalization procedure. We investigated for the first time the isobaric analogue states in the ^{82}Nb and ^{82}Zr, as well as ^{86}Tc and ^{86}Mo. The structure of the low-, intermediate- and high-spin yrast states are very similar for the mirror nuclei. The comparison with the available data indicates good agreement. The prolate-oblate coexistence and mixing found in the structure of the investigated 0^+ states is also present in the non-yrast bands for both A=82 and A=86 nuclei. The present investigation will be extended increasing the dimension of the Excited Vampir many-nucleon basis used for the description of the yrast and non-yrast bands.

References

[1] H. Schatz, A. Aprahamian, V. Barnard, L. Bildsten, A. Cumming, M. Ouellette, T. Rauscher, F.-K. Thielemann, M. Wiescher, Phys. Rev. Lett. 86 (2001) 3471.

[2] I.S. Towner and J.C. Hardy, Phys. Rev. C66 (2002) 035501.

[3] J.C. Hardy and I.S. Towner, Phys. Rev. Lett. 88 (2002) 252501.

[4] J.C. Hardy and I.S. Towner, Eur. Phys. J. A15 (2002) 223.

[5] W.E. Ormand, B.A. Brown, Phys. Rev. C52 (1995) 2455.

[6] H. Sagawa, N. Van Giai, T. Suzuki, Phys. Rev. C53 (1996) 2163.

[7] A. Petrovici, K.W. Schmid, O. Radu, A. Faessler, Nucl. Phys. A747 (2005) 44.

[8] A. Petrovici, K.W. Schmid, A. Faessler, Nucl. Phys. A647 (1999) 197.

[9] A. Petrovici, K.W. Schmid, A. Faessler, J.H. Hamilton, A.V. Ramayya, Progr. Part. Nucl. Phys. 43 (1999) 485.

[10] A. Petrovici, K.W. Schmid, A. Faessler, Nucl. Phys. A665 (2000) 333.

[11] A. Petrovici, Nucl. Phys. A704 (2002) 144c .

[12] A. Petrovici, K.W. Schmid, A. Faessler, Nucl. Phys. A708 (2002) 190.

[13] A. Petrovici, K.W. Schmid, A. Faessler, Nucl. Phys. A710 (2002) 246.

[14] A. Petrovici, K.W. Schmid, A. Faessler, Nucl. Phys. A728 (2003) 396.

[15] F. Becker, A. Petrovici, J. Iwanicki, N. Amzal, W. Korten, K. Hauschild, A. Hurstel, Ch. Theisen, P.A. Butler, R.A. Cunningham, T. Czosnyka, G. de France, J. Gerl, P. Greenlees, K. Helariutta, R.-D. Herzberg, P. Jones, R. Julin, S. Juutinen, H. Kankaanpää, M. Muikku, P. Nieminen, O. Radu, P. Rahkila, Ch. Schlegel, Nucl. Phys. A770 (2006) 107.

[16] A. Petrovici, K.W. Schmid, O. Radu, A. Faessler, J. Phys. G:Nucl. Part. Phys. 32 (2006) 583.

[17] A. Petrovici, K.W. Schmid, O. Radu, A. Faessler, Eur. Phys. J. A28 (2006) 19.

[18] A. Petrovici, Int. J. Mod. Phys. E315, No.7 (2006) 1477.

[19] A. Petrovici, K.W. Schmid, O. Radu, A. Faessler, Nucl. Phys. A799 (2008) 94 .

[20] J. Garces Narro, C. Longour, P.H. Regan, B. Blank, C.J. Pearson, M. Lewitowicz, C. Mieh, W. Gelletly, D. Appelbe, L. Axelsson, A.M. Bruce, W.N. Catford, C. Chandler, R.M. Clark, D.M. Cullen, S. Czajkowski, J.M. Daugas, P. Dessagne, A. Fleury, L. Frankland, J. Giovinazzo, B. Greenhalgh, R. Grzywacz, M. Harder, K.L. Jones, N. Kelsall, T. Kszczot, R.D. Page, A.T. Reed, O. Sorlin, and R. Wadsworth, Phys. Rev. C63 (2001) 044307.

[21] G. Audi, A.H. Wapstra, Nucl. Phys. A595 (1995) 409 .

[22] D. Rudolph, C. Baktash, C.J. Gross, W.Satula, R. Wyss, L.Birriel, M. Devlin, H.-Q. Jin, D.R. LaFosse, F. Lerma, J.X. Saladin, D.G. Sarantities, G.N. Sylvan, S.L. Tabor, D.F. Winchell, V.Q. Wood, C.H. Yu, Phys. Rev. C56 (1997) 98.

[23] D. Rudolph, C.J. Gross, Y.A. Akovali, C. Baktash, J. Döring, F.E. Durham, P.-F. Hua, G.D. Johns, M. Korolija, D.R. LaFosse, I.Y. Lee, A.O. Macchiavelli, W. Rathbun, D.G. Sarantities, D.W. Stracener, S.L. Tabor, A.V. Afanasjev, I. Ragnarsson, Phys. Rev. C54 (1996) 117.

Table 1. $B(E2; I \to I-2)$ values (in e^2fm^4) for the yrast states of the nucleus ^{82}Zr and ^{82}Nb

$I^\pi[\hbar]$	^{82}Zr Experiment	^{82}Zr Theory	^{82}Nb Theory
2^+	2328^{+1058}_{-1058}	1351	1291
4^+	2328^{+1058}_{-1058}	1992	1913
6^+	1672^{+395}_{-395}	2166	2070
8^+	2539^{+1058}_{-1058}	2174	1995
10^+	2328^{+635}_{-635}	2129	1889
12^+	1926^{+486}_{-486}	1974	1867
14^+	1904^{+634}_{-634}	1733	1753
16^+	> 621	1472	1596
18^+		809	
20^+		808	

Table 2. $B(E2; I \to I-2)$ values (in e^2fm^4) for the yrast states of the nucleus ^{82}Zr and ^{86}Mo

$I^\pi[\hbar]$	^{82}Zr Experiment	^{82}Zr Theory	^{86}Mo Theory
2^+	2328^{+1058}_{-1058}	1351	875
4^+	2328^{+1058}_{-1058}	1992	1277
6^+	1672^{+395}_{-395}	2166	1298
8^+	2539^{+1058}_{-1058}	2174	1288
10^+	2328^{+635}_{-635}	2129	1176
12^+	1926^{+486}_{-486}	1974	1053
14^+	1904^{+634}_{-634}	1733	908
16^+	> 621	1472	692
18^+		809	492
20^+		808	

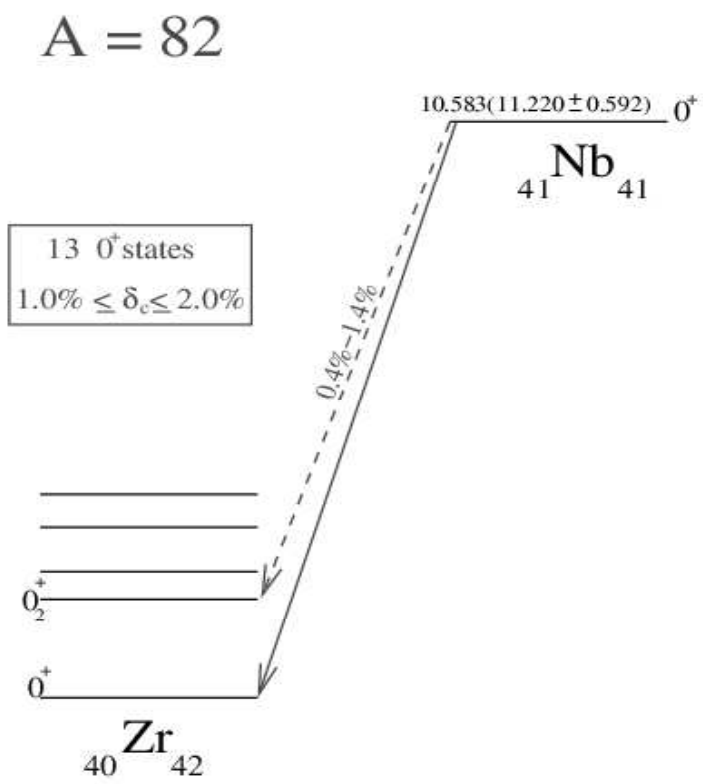

Fig. 1. The theoretical spectrum of the lowest 0^+ states in ^{82}Zr obtained whithin the *complex* Excited Vampir approach and the results on superallowed Fermi β decay of ^{82}Nb.

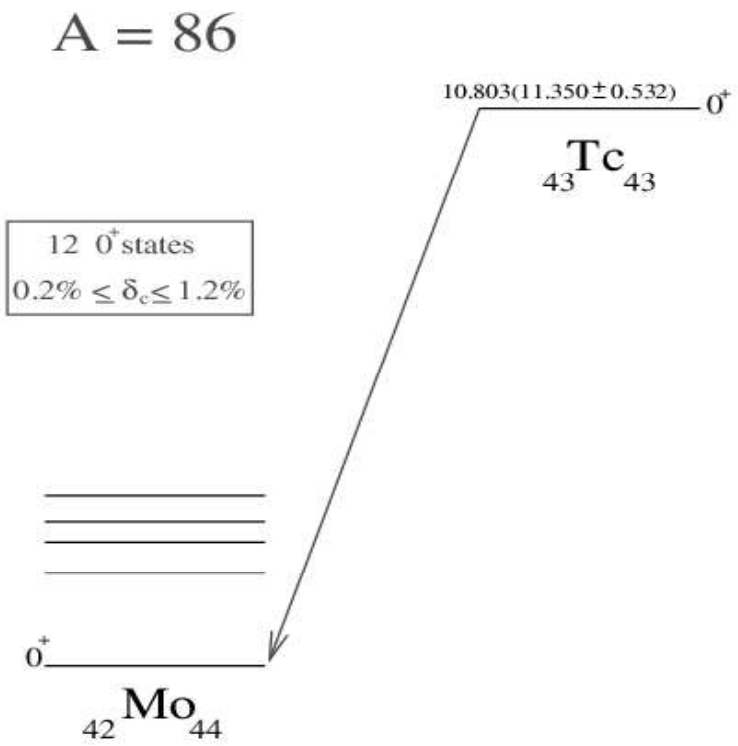

Fig. 2. The same as in Fig. 1, but for the A=86 T=1 nuclei.

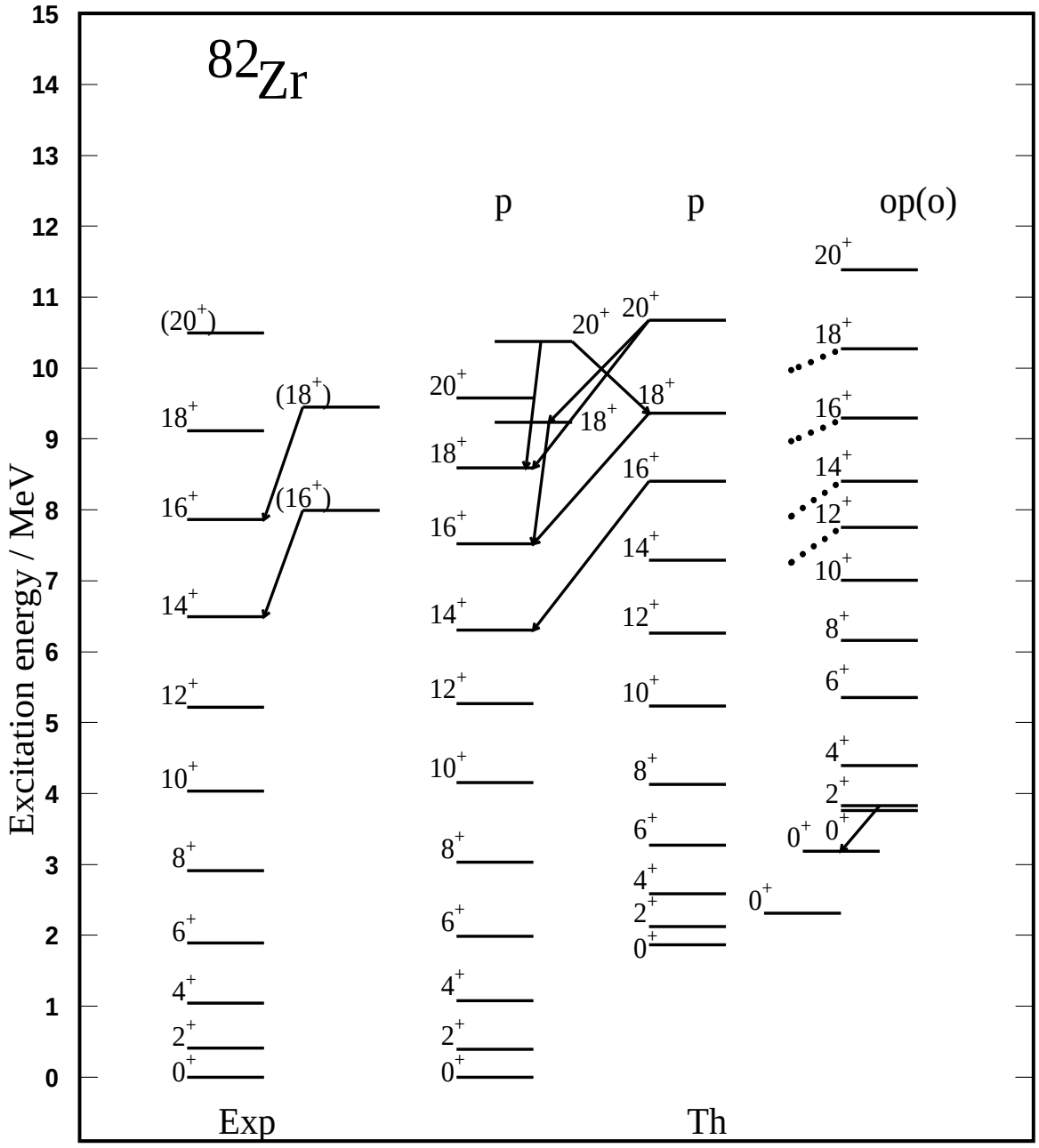

Fig. 3. The theoretical spectrum of ^{82}Zr obtained whithin the *complex* Excited Vampir approach is compared with the available data [22].

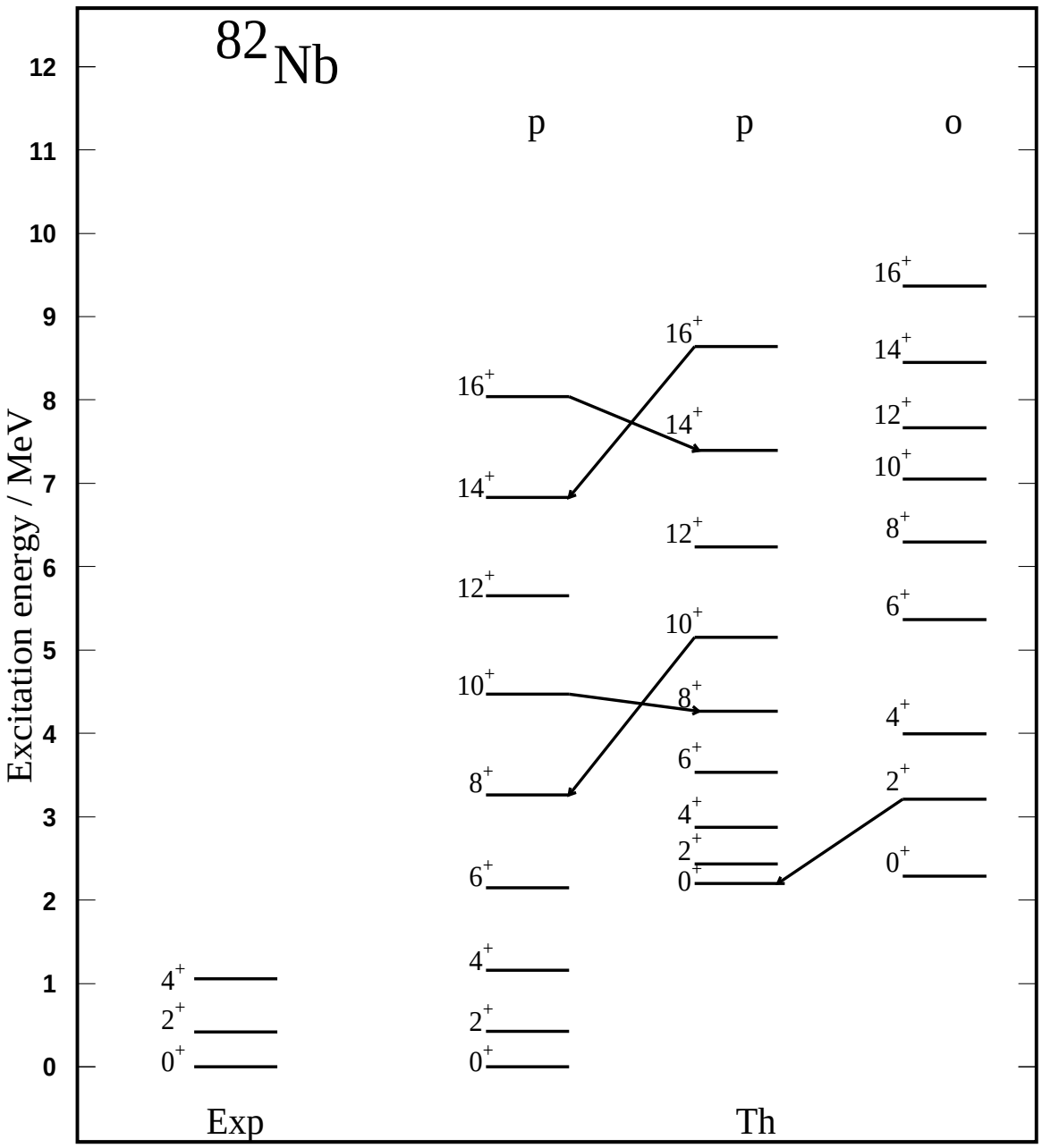

Fig. 4. The same as in Fig. 3, but for the ^{82}Nb nucleus.

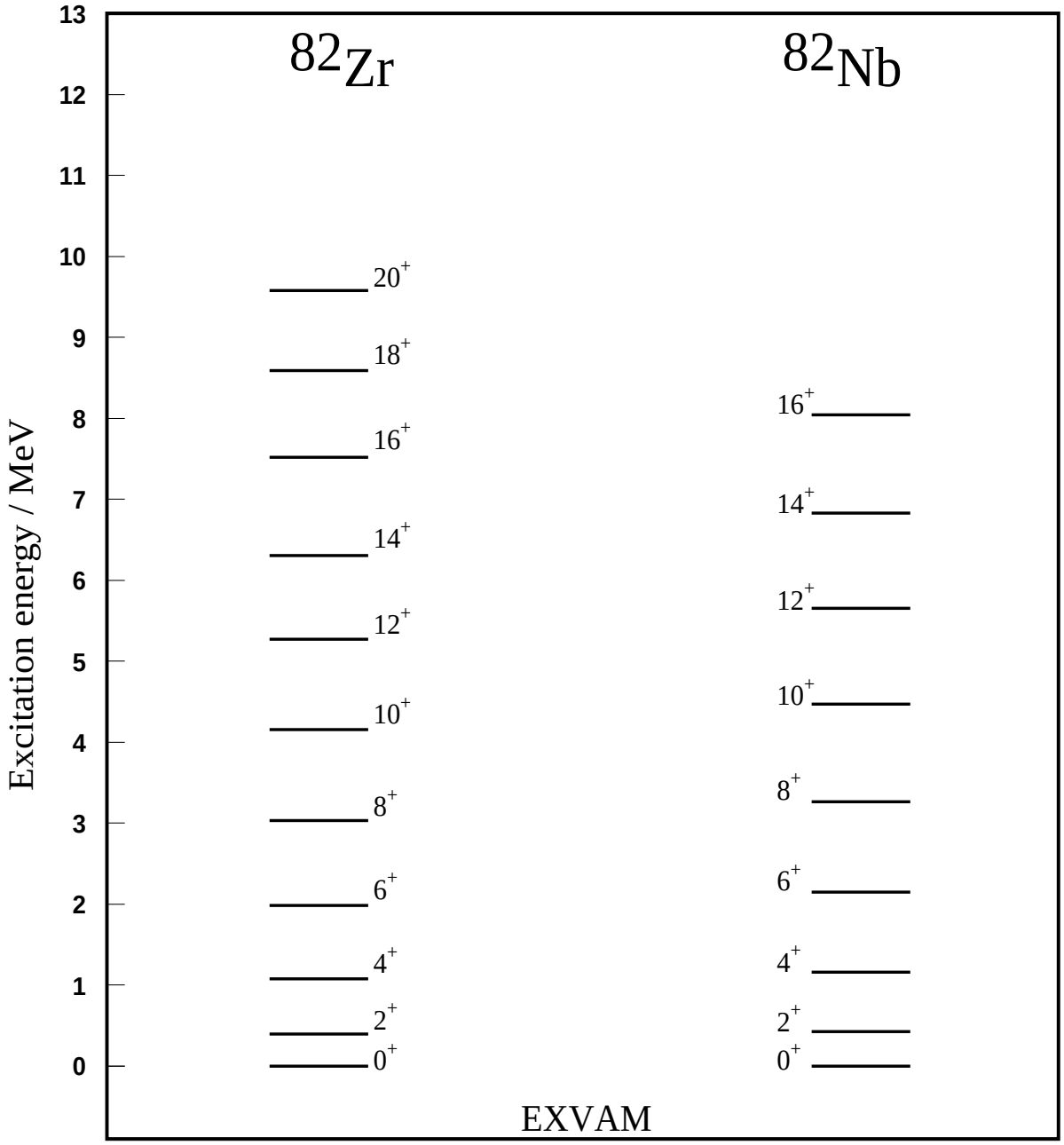

Fig. 5. A direct comparison of the yrast positive-parity spectrum of the mirror nuclei ^{82}Zr and ^{82}Nb.

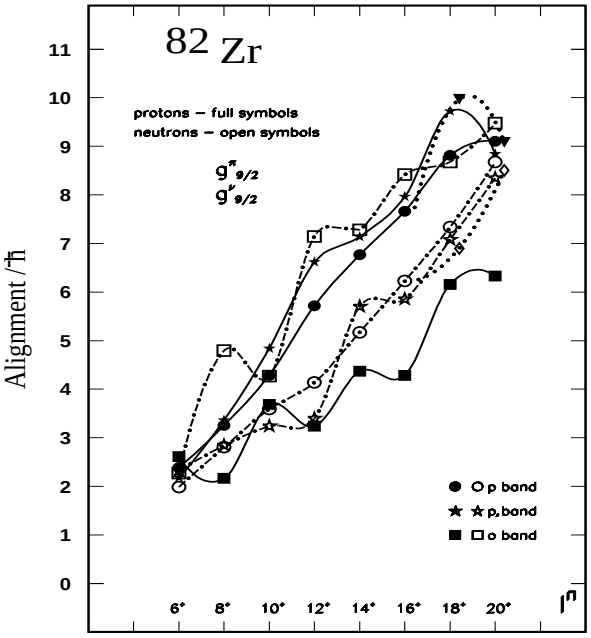

Fig. 6. The alignment plot for the ^{82}Zr bands presented in Fig. 3.

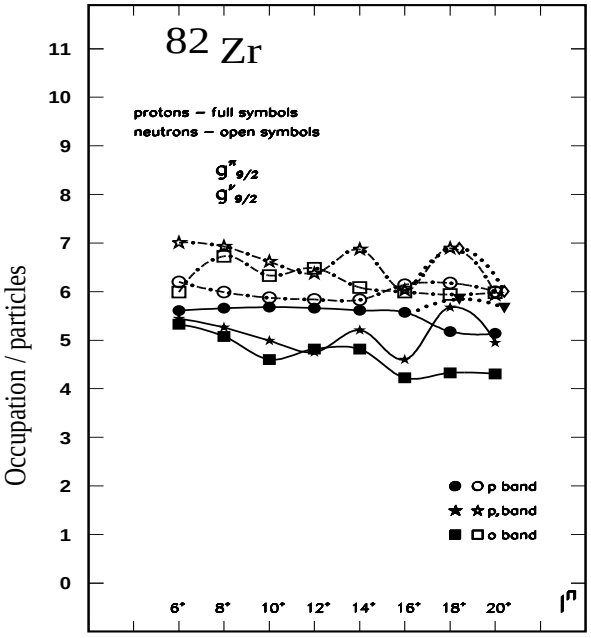

Fig. 7. The occupation of the spherical $0g_{9/2}$ orbital for the ^{82}Zr states presented in Fig. 3.

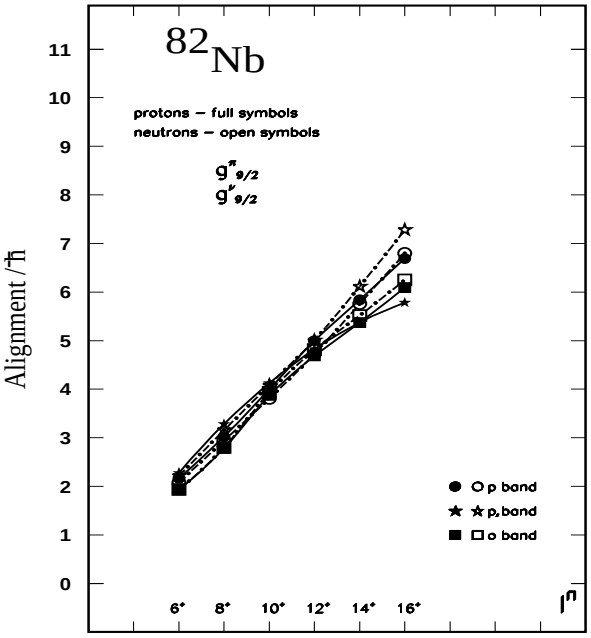

Fig. 8. The same as in Fig. 6, but for the ^{82}Nb nucleus.

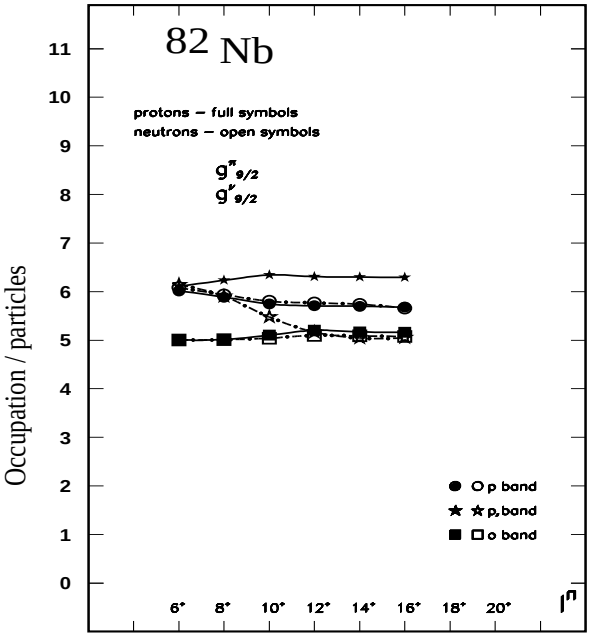

Fig. 9. The same as in Fig. 7, but for the ^{82}Nb nucleus.

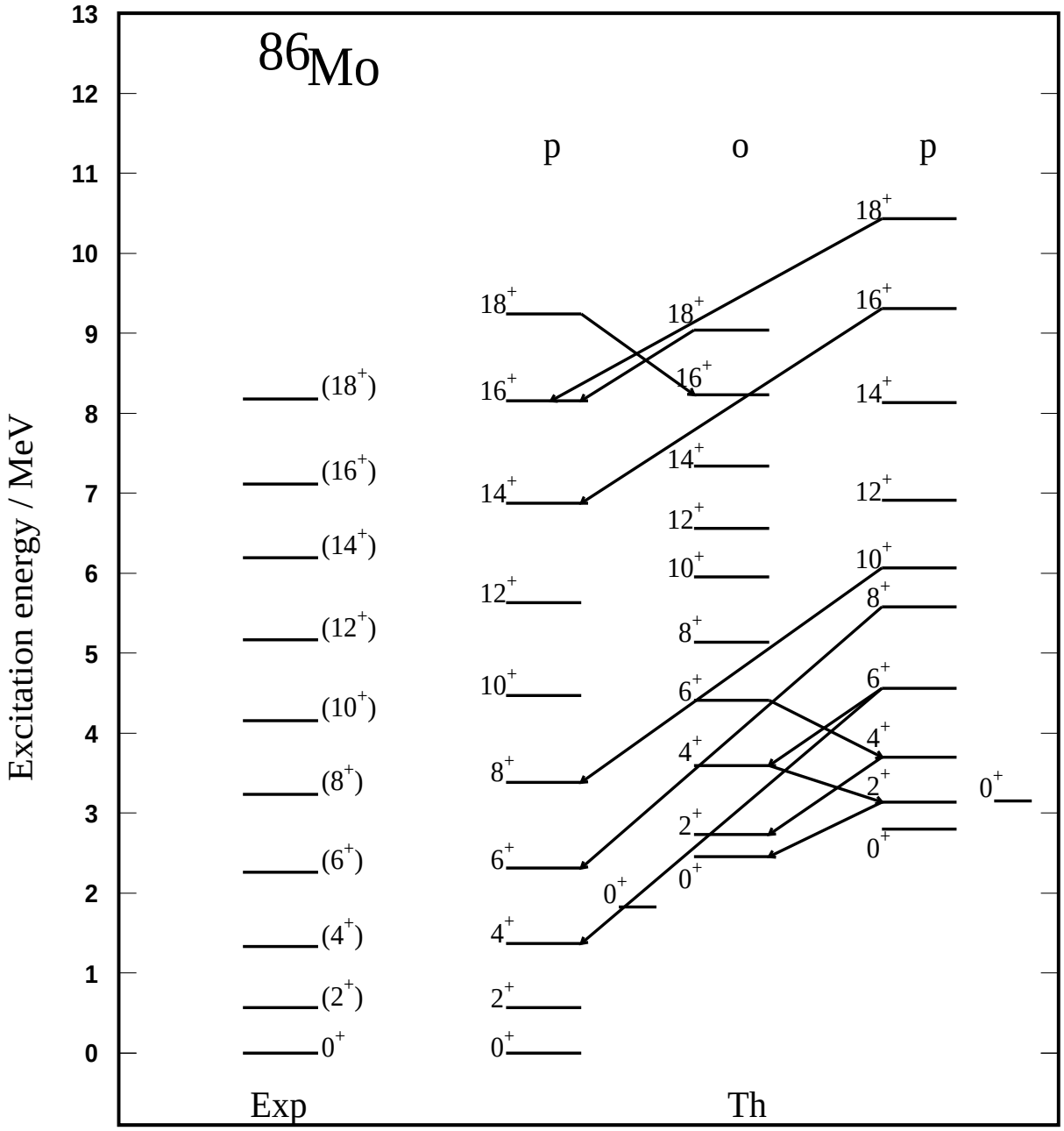

Fig. 10. The same as in Fig. 3, but for the ^{86}Mo nucleus.

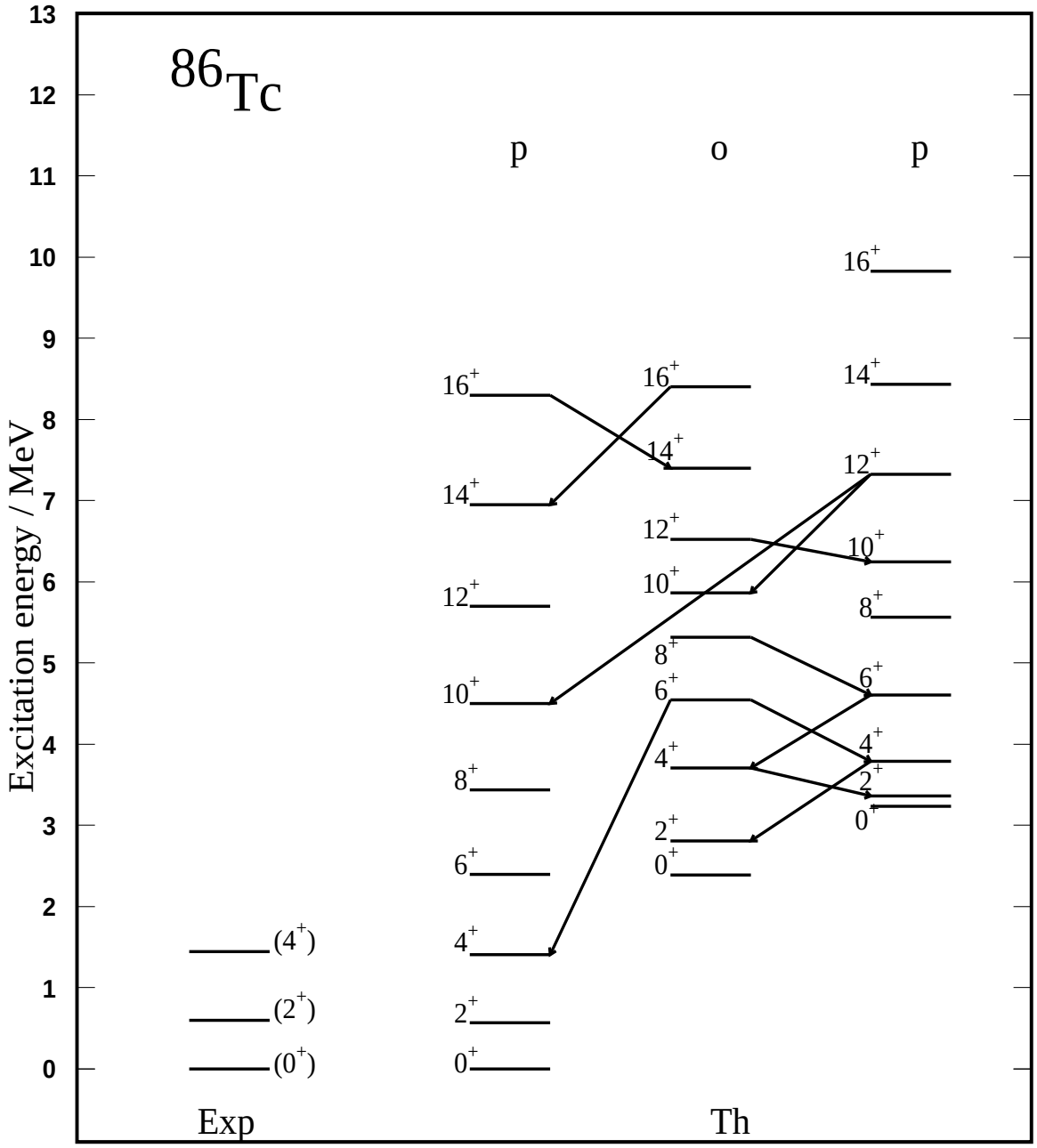

Fig. 11. The same as in Fig. 10, but for the ^{86}Tc nucleus.

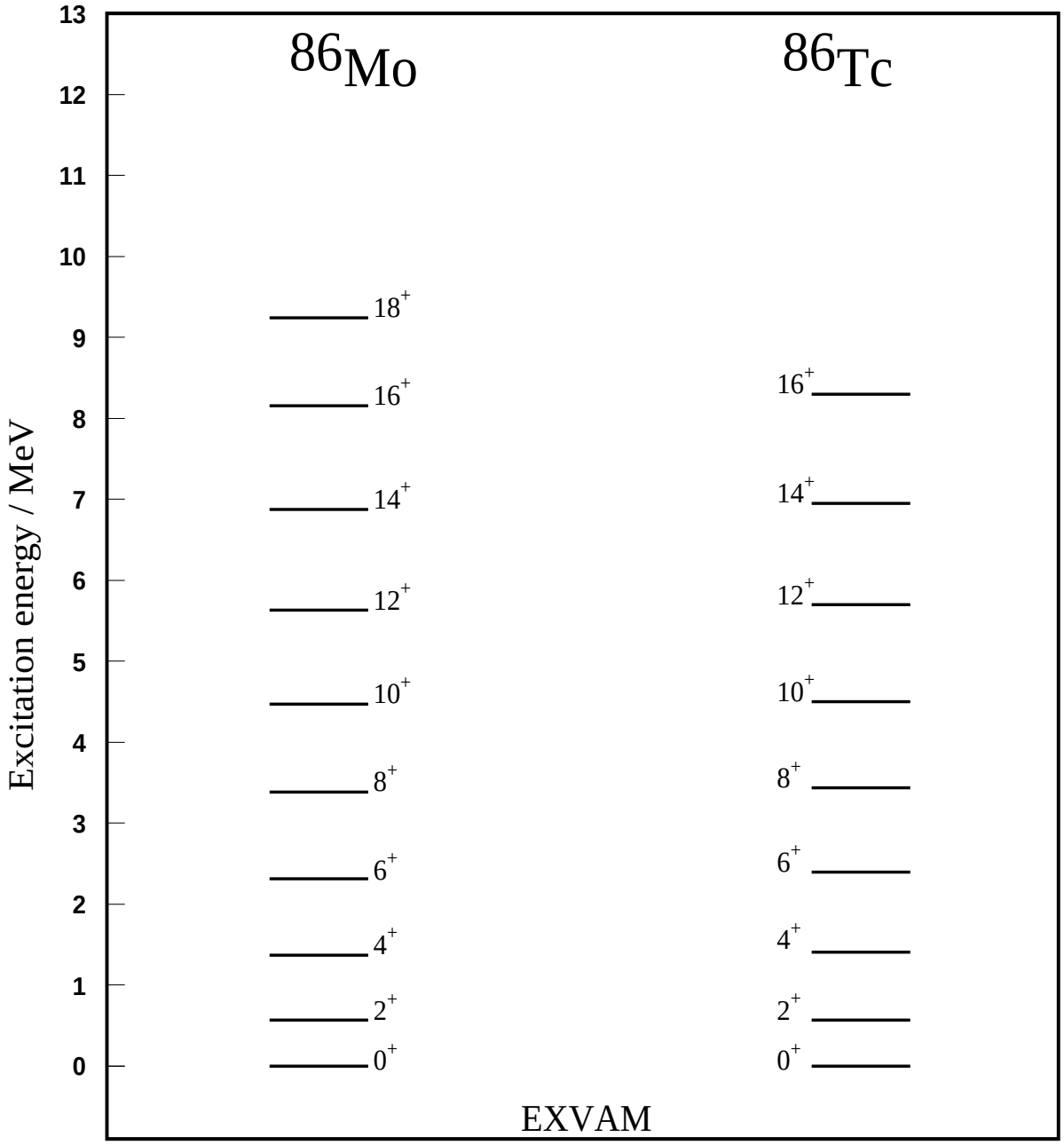

Fig. 12. The same as in Fig. 5, but for the A=86 mirror nuclei.

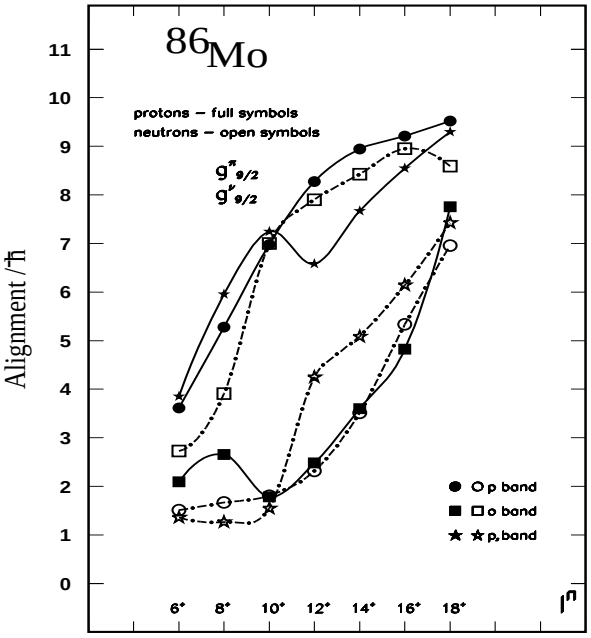

Fig. 13. The same as in Fig. 6, but for the ^{86}Mo nucleus.

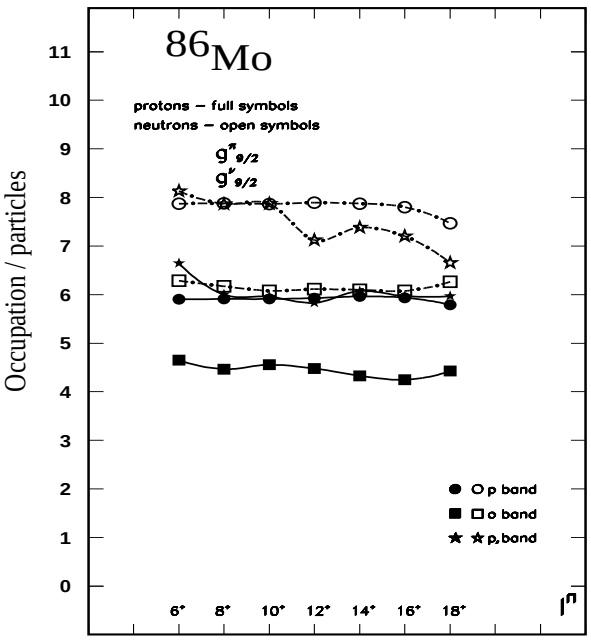

Fig. 14. The same as in Fig. 7, but for the ^{86}Mo nucleus.

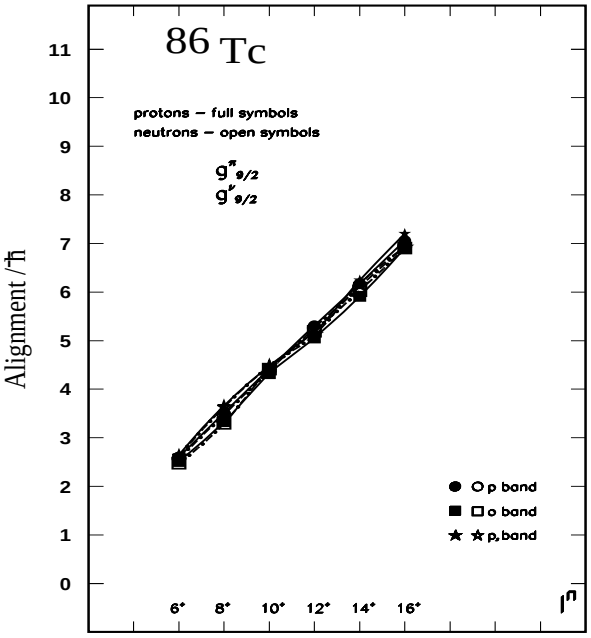

Fig. 15. The same as in Fig. 13, but for the ^{86}Tc nucleus.

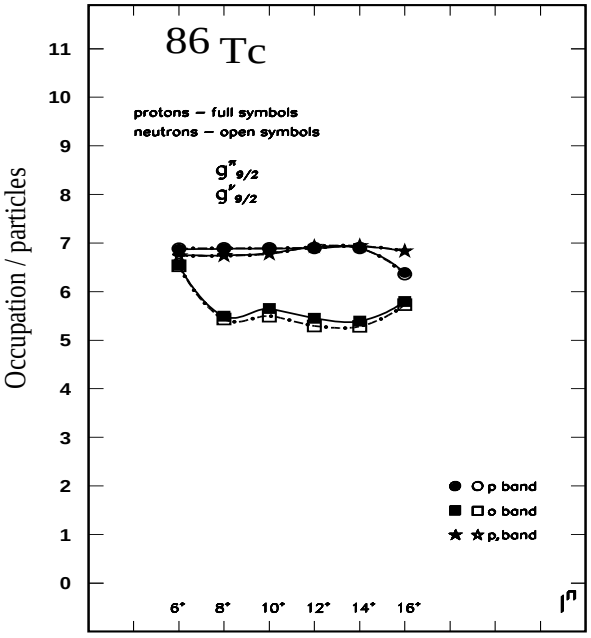

Fig. 16. The same as in Fig. 14, but for the ^{86}Tc nucleus.